Multiple Scattering Parameterization in Thermal Infrared Radiative Transfer

QIANG FU

Atmospheric Science Program, Dalhousie University, Halifax, Nova Scotia, Canada

K. N. LIOU

Department of Meteorology/CARSS, University of Utah, Salt Lake City, Utah

M. C. CRIBB

Atmospheric Science Program, Dalhousie University, Halifax, Nova Scotia, Canada

T. P. CHARLOCK

NASA Langley Research Center, Hampton, Virginia

A. GROSSMAN

Atmospheric Sciences Division, Lawrence Livermore National Laboratories, Livermore, California

(Manuscript received 30 October 1996, in final form 1 May 1997)

ABSTRACT

A systematic formulation of various radiative transfer parameterizations is presented, including the absorption approximation (AA), δ-two-stream approximation (D2S), δ-four-stream approximation (D4S), and δ-two- and four-stream combination approximation (D2/4S), in a consistent manner for thermal infrared flux calculations. The D2/4S scheme uses a source function from the δ-two-stream approximation and evaluates intensities in the four-stream directions. A wide range of accuracy checks for monochromatic emissivity of a homogeneous layer and broadband heating rates and fluxes in nonhomogeneous atmospheres is performed with respect to the ''exact'' results computed from the δ-128-stream scheme for radiative transfer. The computer time required for the calculations using different radiative transfer parameterizations is compared. The results pertaining to the accuracy and efficiency of various radiative transfer approximations can be utilized to decide which approximate method is most appropriate for a particular application. In view of its overall high accuracy and computational economy, it is recommended that the D2/4S scheme is well suited for GCM and climate modeling applications.

1. Introduction

General circulation models (GCMs) are key elements of modern climate research and the effort to accurately predict climate change. Since the major energy sources and sinks for the global climate system are solar and terrestrial radiation, modeling and prediction of climate require an accurate treatment of radiative transfer processes in GCMs. At the same time, the computational burden associated with radiation calculations in GCMs is such that efficient techniques are essential. The object of the radiative transfer parameterization in atmospheric numerical models is to therefore provide an accurate and efficient method to calculate radiative fluxes and heating rates during the course of model integration (Stephens 1984). An accurate and fast radiation model is also required in conjunction with the retrieval of atmospheric radiative fluxes based on satellite data (Charlock and Alberta 1996).

Efficient treatments for the transfer of solar radiation have been extensively studied. Among the simplest and most widely used approximations are the (δ-) two-stream techniques (see, e.g., Meador and Weaver 1980), whose accuracies have been comprehensively examined by King and Harshvardhan (1986). To achieve higher accuracy within a wide range of atmospheric conditions, the (δ-) four-stream approximation was proposed (Liou 1974; Cuzzi et al. 1982; Liou et al. 1988). The accuracy of the δ-four-stream scheme has been checked in both homogeneous and nonhomogeneous atmospheres (Liou et al. 1988; Fu 1991; Shibata and Uchiyama 1992). By contrast, little attention has been given to methods of

Corresponding author address: Prof. Qiang Fu, Dept. of Oceanography, Dalhousie University, Halifax, NS B3H 4J1, Canada.
E-mail: qfu@atm.dal.ca

treating scattering in the presence of thermal emission (Toon et al. 1989).

In atmospheric models, computation of the infrared fluxes in a multiple scattering atmosphere is usually highly simplified. One commonly used approximation, as discussed by Stephens (1984), is to neglect scattering and consider cloud and aerosol particles as purely absorbing particles. Recently, the δ-two-stream (Stephens et al. 1990; Stackhouse and Stephens 1991; Ritter and Geleyn 1992) and δ-four-stream (Fu and Liou 1993) approximations have been applied to infrared as well as solar spectra. However, the accuracy of various transfer methodologies for the calculation of infrared fluxes and heating rates has not been examined sufficiently. Furthermore, it is useful to compare different radiative transfer approximations in terms of both accuracy and computational efficiency because these two factors are usually competing against each other.

This paper is intended to provide a systematic discussion of the treatment of the multiple scattering process for the transfer of thermal infrared radiation. Section 2 introduces various approximations in a consistent manner. In section 3, we present a wide range of accuracy checks for these approximations in calculating monochromatic emissivity of a homogeneous layer as well as broadband atmospheric radiative heating rates and fluxes. A discussion of the results follows in section 4, including recommendations for using these approximations based on accuracy and computer time requirements. Finally, a summary and conclusions are given in section 5.

2. Radiative transfer in the thermal infrared

Since we are concerned with flux calculations, we shall begin with the azimuth-averaged equation governing the transfer of diffuse infrared intensity, I, in plane-parallel atmospheres and local thermodynamic equilibrium given by (e.g., Liou 1992)

$$\mu \frac{dI(\tau, \mu)}{d\tau} = I(\tau, \mu) - \frac{\tilde{\omega}}{2} \int_{-1}^{1} I(\tau, \mu') P(\mu, \mu')\, d\mu' - (1 - \tilde{\omega}) B(T), \tag{2.1}$$

where $\mu = \cos\theta$, θ is the zenith angle, τ the normal optical depth, $\tilde{\omega}$ the single-scattering albedo, and $B(T)$ the blackbody intensity at temperature T. The azimuth-independent phase function is defined as

$$P(\mu, \mu') = \frac{1}{2\pi} \int_{0}^{2\pi} P(\cos\Theta)\, d\phi, \tag{2.2}$$

where $P(\cos\Theta)$ is the scattering phase function and the cosine of the scattering angle is defined by $\cos\Theta = \mu\mu' + (1 - \mu^2)^{1/2}(1 - \mu'^2)^{1/2} \cos\phi$, with ϕ the azimuthal angle.

Consider a homogeneous layer with respect to the single-scattering albedo and the phase function. If this layer is nonisothermal, information about the optical depth dependence of the Planck function is needed. A linear-in-optical-depth variation of the Planck function is commonly adopted for this purpose (Wiscombe 1976; Tsay et al. 1989; Toon et al. 1989). Using a different approach, we have approximated the Planck function exponentially in optical depth in the form (Fu 1991; Fu and Liou 1993)

$$B[T(\tau)] = \alpha e^{\beta\tau}, \tag{2.3}$$

where $\alpha = B_0$ and $\beta = (1/\tau_1) \ln(B_1/B_0)$, with B_0 and B_1 the Planck functions for the temperature at the top and bottom of the layer, respectively, and τ_1 the optical depth of the layer. Kylling and Stamnes (1992) introduced and tested an exponential-linear approximation, which is also superior to a linear approximation.

In the following, we will introduce various approximations for infrared radiative transfer parameterizations in a consistent manner.

a. Absorption approximation

This approximation neglects the scattering effects. The basic radiative transfer equation can then be simplified in the form

$$\mu \frac{dI(\tau, \mu)}{d\tau} = (1 - \tilde{\omega}) I(\tau, \mu) - (1 - \tilde{\omega}) B(T). \tag{2.4}$$

This equation can be derived from Eq. (2.1) by assuming that either the radiative intensity is isotropic or the scattering phase function is the δ function. It is also valid when the single-scattering albedo is zero. Because of the very strong gaseous absorption outside the atmospheric window (8–13 μm), the radiation effect of cloud and aerosol particles is normally confined to the window spectral range where the scattering efficiency of these particles is much smaller than that in the visible (Fouquart et al. 1990). Also, the distribution of the infrared radiation sources is much more isotropic compared to the shortwave, thus reducing the role of multiple scattering. Although the scattering effect of cloud and aerosol particles is generally small in the infrared, it cannot be neglected in the window region (Toon et al. 1989). This is the case for high cirrus clouds in which scattering may play an important role in the IR radiative energy budget (Liou 1986). It has been shown that the reflection of the infrared flux from the base of a cold cloud over a warm surface leads to a cloud emissivity substantially larger than one (Stephens 1984; Fu and Liou 1993).

Using Eq. (2.3), the solution to Eq. (2.4) for a homogeneous layer can be written as

$$I(0, \mu) = I(\tau_1, \mu) e^{-(1-\tilde{\omega})\tau_1/\mu} + \frac{1 - \tilde{\omega}}{\mu\beta - 1 + \tilde{\omega}} \times [B_1 e^{-(1-\tilde{\omega})\tau_1/\mu} - B_0], \tag{2.5a}$$

$$I(\tau_1, -\mu) = I(0, -\mu) e^{-(1-\tilde{\omega})\tau_1/\mu} + \frac{1 - \tilde{\omega}}{\mu\beta + 1 - \tilde{\omega}} \times [B_1 - B_0 e^{-(1-\tilde{\omega})\tau_1/\mu}], \tag{2.5b}$$

where $\mu > 0$ and μ and $-\mu$ are associated with the upward and downward intensities, respectively. In Eq. (2.5), $I(\tau_1, \mu)$ and $I(0, -\mu)$ are, respectively, the inward intensities at the bottom and top surfaces.

For infrared radiation, diffuse transmission can be computed from transmission by using a diffusivity factor of 1.66 (e.g., Goody 1964). Therefore we can evaluate radiative intensities at $\mu = 1/1.66$ based on Eq. (2.5) to obtain the upward and downward fluxes:

$$F^+(0) = \pi I(0, 1/1.66), \tag{2.6a}$$

$$F^-(\tau_1) = \pi I(\tau_1, -1/1.66). \tag{2.6b}$$

For application to real atmospheres, we may divide the entire atmosphere into a number of suitable homogeneous layers. We first evaluate the downward intensity at each atmospheric level by working downward from the top of the atmosphere toward the surface, then use the surface boundary condition and evaluate the upward intensity by working backward through the layers. Here we may assume that the downward intensity at the top of the atmosphere is zero. For a surface with an emissivity of ε, the surface boundary condition is

$$I_S(1/1.66) = (1 - \varepsilon)I_S(-1/1.66) + \varepsilon B(T_S), \tag{2.7}$$

where T_S is the surface temperature, and $I_S(1/1.66)$ and $I_S(-1/1.66)$ are the upward and downward intensities at the surface, respectively.

The thermal infrared scattering can be significant at the earth's surface (Salisbury and D'Aria 1992), especially over deserts (Prabhakara and Dalu 1976), and is a factor in the remote sensing of SST (Smith et al. 1996). The absorption approximation (AA) method considers the surface scattering explicitly through the boundary condition (2.7).

b. Two-stream approximation

The simplest method to treat the multiple scattering process is the two-stream scheme, which has been widely used. The discrete-ordinates two-stream approximation can be obtained from Eq. (A.4) in the appendix by setting $n = N = 1$. In this case, the Gauss quadrature and weight are $\mu_1 = \sqrt{3}/3$ and $a_1 = 1$. The use of Gauss quadrature in the discrete-ordinates method makes phase function renormalization unnecessary, implying that energy is conserved (Stamnes et al. 1988). However, the relation between the flux and intensity assumed in the two-stream approximation, that is, $F^{\pm}(\tau) = 2\pi\mu_1 I(\tau, \pm\mu_1)$, is physically incorrect for an isotropic source. Toon et al. (1989) showed that the Eddington approximation also leads to physically incorrect results.

For infrared radiative transfer, we modify the discrete-ordinates two-stream approximation by using $F^{\pm}(\tau) = \pi I(\tau, \pm\mu_1)$ with $\mu_1 = 1/1.66$, which is consistent with the absorption approximation in the limit of no scattering. Furthermore, the phase function $P(\mu_1, \pm\mu_1) = 1 \pm g$ should be used in the two-stream scheme because the absorption approximation is also exact when g = 1. In view of these considerations, we can approximate the integral in Eq. (2.1) by $I(\tau, -\mu_1)P(\mu, -\mu_1) + I(\tau, \mu_1)P(\mu, \mu_1)$. Substituting $\pm\mu_1$ for μ and $P(\mu_1, \pm\mu_1) = 1 \pm g$ in the result and multiplying it by π, we have

$$\frac{\partial F^+}{\partial \tau} = r_1 F^+ - r_2 F^- - S, \tag{2.8a}$$

$$\frac{\partial F^-}{\partial \tau} = r_2 F^+ - r_1 F^- + S, \tag{2.8b}$$

where

$$r_1 = D\left[1 - \frac{\tilde{\omega}}{2}(1 + g)\right], \tag{2.9}$$

$$r_2 = D\frac{\tilde{\omega}}{2}(1 - g), \tag{2.10}$$

$$S = D(1 - \tilde{\omega})\pi B[T(\tau)], \tag{2.11}$$

with $D = 1.66$. By setting $D = 2$, we have the hemispheric mean two-stream scheme (Toon et al. 1989). Both the hemispheric mean and modified two-stream approximations are energy conserving as well as providing a correct relation between the flux and intensity for an isotropic radiation field. However, the modified two-stream approximation is more accurate than the hemispheric mean two-stream scheme because the μ_1 used is related to the 1.66 diffusivity factor. As demonstrated in previous studies (e.g., Goody 1964; Stephens 1984; Liou 1992), using $D = 1.66$ in $F^{\pm}(\tau) = \pi I(\tau, \pm 1/D)$ gives optimum accuracy in the limit of no scattering. Note that Eq. (2.8) also reduces to the absorption approximation when $g = 1$. We regard the present modified two-stream approximation as the most appropriate for infrared transfer among two-stream techniques.

Using Eq. (2.3) for the approximation of the Planck function, the general solution for Eq. (2.8) can be expressed by

$$F^+(\tau) = g_1 e^{-k(\tau_1 - \tau)} + g_2 R e^{-k\tau} + Z_+, \tag{2.12a}$$

$$F^-(\tau) = g_1 R e^{-k(\tau_1 - \tau)} + g_2 e^{-k\tau} + Z_-, \tag{2.12b}$$

where

$$k = (r_1^2 - r_2^2)^{1/2}, \tag{2.13a}$$

$$R = \frac{r_1 - k}{r_2} = \frac{r_2}{r_1 + k}, \tag{2.13b}$$

$$Z_{\pm} = \frac{S}{k^2 - \beta^2}(r_1 \pm \beta + r_2), \tag{2.13c}$$

and the coefficients $g_{1,2}$ are to be determined from radiation boundary conditions.

Equation (2.12) for a single homogeneous layer can be extended to a nonhomogeneous atmosphere by dividing the atmosphere into a number of appropriate ho-

mogeneous layers. By applying the boundary conditions and the internal continuity requirements, a matrix can be formulated and inverted to obtain the fluxes throughout the atmosphere. Toon et al. (1989) have utilized a standard tridiagonal technique for matrix inversion. This technique is made numerically stable by including scaling transformation and pivoting (Stamnes et al. 1988; Kylling et al. 1995). The surface boundary condition for the two-stream approximation is

$$F_s^+ = (1 - \varepsilon)F_s^- + \varepsilon\pi B(T_s). \tag{2.14}$$

c. Four-stream approximation

The four-stream approximation for both solar and infrared radiative transfer has been discussed in detail by Liou et al. (1988), Fu (1991), and Fu and Liou (1993). A brief description of this approximation is given below.

From Eq. (A.4), the four-stream approximation can be obtained by setting $n = 2$ and $N = 3$. The quadrature formula that Sykes (1951) referred to as double Gauss is employed, which leads to $\mu_1 = 0.2113248$, $\mu_2 = 0.7886752$, $a_1 = 0.5$, and $a_2 = 0.5$ in the four-stream approximation (Fu 1991). We note that $\Sigma_{j=1}^{2} a_j\mu_j = 0.5$ so that the double Gauss quadrature provides an exact relation between the flux and intensity for an isotropic source. This introduces a distinct advantage over the Gauss quadrature in which $\Sigma_{j=1}^{2} a_j\mu_j = 0.52127$. In the four-stream approximation, the Planck function is again expressed in terms of the optical depth in an exponential form.

Like various two-stream approximations, an analytic solution for the four-stream approximation can be derived explicitly. Using the four-stream approximation, the flux distribution can be computed by dividing the atmosphere into a number of homogeneous layers. In the resulting matrix formulation, one-third of the elements in the diagonal band of the coefficient matrix are found to be zero. We have developed a numerically stable technique to solve the system of linear equations (Fu and Liou 1993). Compared with the standard routines available in the IMSL or LAPACK software libraries for solving a general banded matrix, our program is significantly faster (Fu 1991). This is because the zero elements within the diagonal band matrix were explicitly considered.

The surface boundary condition for the four-stream approximation is given by

$$I_s(\mu_i) = 2(1 - \varepsilon)\sum_{j=1}^{2} a_j\mu_j I_s(-\mu_j) + \varepsilon B(T_s), \quad i = 1, 2. \tag{2.15}$$

d. Two- and four-stream combination

For a homogeneous layer with an optical thickness, τ_1, we can solve Eq. (2.1) formally to obtain ($\mu > 0$):

$$I(0, \mu) = I(\tau_1, \mu)e^{-\tau_1/\mu} + \int_0^{\tau_1} M(\tau', \mu)e^{-\tau'/\mu}\, d\tau'/\mu, \tag{2.16a}$$

$$I(\tau_1, -\mu) = I(0, -\mu)e^{-\tau_1/\mu} + \int_0^{\tau_1} M(\tau', -\mu)e^{-(\tau_1-\tau')/\mu}\, d\tau'/\mu, \tag{2.16b}$$

where $M(\tau', \pm\mu)$ is the source function associated with multiple scattering and emission, which can be written as

$$M(\tau, \pm\mu) = \frac{\tilde{\omega}}{2}\int_{-1}^{1} I(\tau, \mu')P(\pm\mu, \mu')\, d\mu' + (1 - \tilde{\omega})B[T(\tau)]. \tag{2.17}$$

The Planck function is related to the optical depth via Eq. (2.3).

In the two- and four-stream combination method, we first solve the source function by using the two-stream scheme. Then we use Eq. (2.16) to evaluate intensities in the four-stream directions. The fluxes can then be obtained following Eq. (A.5). Here, the double Gauss points and weights are used in the four-stream intensity and flux calculations.

Using the two-stream approximation, the source functions corresponding to upward and downward directions are given by

$$M(\tau, 1/D) = Ge^{-k(\tau_1-\tau)} + He^{-k\tau} + \zeta B[T(\tau)], \tag{2.18a}$$

$$M(\tau, -1/D) = Je^{-k(\tau_1-\tau)} + Ke^{-k\tau} + \eta B[T(\tau)], \tag{2.18b}$$

where

$$G = \frac{g_1}{\pi}(1 - k/D), \tag{2.19}$$

$$H = \frac{g_2}{\pi}R(1 + k/D), \tag{2.20}$$

$$J = \frac{g_1}{\pi}R(1 + k/D), \tag{2.21}$$

$$K = \frac{g_2}{\pi}(1 - k/D), \tag{2.22}$$

$$\zeta = (1 - \tilde{\omega})\left(D\tilde{\omega}\frac{r_1 + r_2 + g\beta}{k^2 - \beta^2} + 1\right), \tag{2.23}$$

$$\eta = (1 - \tilde{\omega})\left(D\tilde{\omega}\frac{r_1 + r_2 - g\beta}{k^2 - \beta^2} + 1\right), \tag{2.24}$$

where $D = 1.66$ based on the modified two-stream scheme and $D = 2$ based on the hemispheric mean two-stream scheme.

Since multiple scattering is not a dominant process in the infrared radiative transfer, it suffices to evaluate the source function by using the two-stream approximation. Replacing $M(\tau', \pm\mu)$ in Eq. (2.16) by $M(\tau', \pm 1/D)$ from Eq. (2.18), we have the intensity at a given μ as follows:

$$I(0, \mu) = I(\tau_1, \mu)e^{-\tau_1/\mu} + \frac{G}{k\mu - 1}(e^{-\tau_1/\mu} - e^{-k\tau_1}) + \frac{H}{k\mu + 1}[1 - e^{-\tau_1(k+1/\mu)}] + \frac{\zeta}{1 - \mu\beta}[B(0) - B(\tau_1)e^{-\tau_1/\mu}], \quad (2.25a)$$

$$I(\tau_1, -\mu) = I(0, -\mu)e^{-\tau_1/\mu} + \frac{J}{k\mu + 1}[1 - e^{-\tau_1(k+1/\mu)}] + \frac{K}{k\mu - 1}(e^{-\tau_1/\mu} - e^{-\tau_1 k}) + \frac{\eta}{1 + \mu\beta}[B(\tau_1) - B(0)e^{-\tau_1/\mu}], \quad (2.25b)$$

where $\mu = 0.2113248$ and 0.7886752 in the four-stream calculation.

At infrared wavelengths, Fu (1991) has shown that radiative fluxes can be accurately evaluated from intensities using a two-ordinate double Gauss quadrature, that is, four-stream approximation, in the limit of no scattering. For this reason, there is little advantage gained by using D = 1.66 instead of using $D = 2$ in the two- and four-stream combination approach. Numerical studies show that results from D2/4S with $D = 2$ are similar to those with $D = 1.66$. Here we adopt $D = 2$ in D2S/4S. This is because the hemispheric mean two-stream scheme is more consistent with our four-stream scheme by noting that $(\mu_1 + \mu_2)/2 = 1/D$.

The two- and four-stream combination approach seems to be promising because it may incorporate the speed of the two-stream approximation and the accuracy of the four-stream approximation. This approach is developed based on the source function technique proposed by Toon et al. (1989).

For application to nonhomogeneous atmospheres, we may first solve the two-stream approximation by dividing the atmosphere into a number of homogeneous layers. Downward intensities can then be computed at each level by applying Eq. (2.25b) from the top of the atmosphere progressively to the surface. Using the surface boundary condition given by Eq. (2.15), upward intensities can subsequently be obtained from Eq. (2.25a) through the layers. After the intensities at each level for four angles are determined, upward and downward fluxes can then be evaluated using the quadrature.

Finally, to incorporate the forward peak contribution in multiple scattering, we can use the similarity principle (or the so-called δ-function adjustment) for radiative transfer to adjust the optical depth, single-scattering albedo, and expansion coefficients of the phase function in the form (Joseph et al. 1976; Liou et al. 1988)

$$\tau' = \tau(1 - f\tilde{\omega}), \quad (2.26a)$$

$$\tilde{\omega}' = (1 - f)\tilde{\omega}/(1 - f\tilde{\omega}), \quad (2.26b)$$

$$\tilde{\omega}'_\ell = [\tilde{\omega}_\ell - f(2\ell + 1)]/(1 - f), \quad (2.26c)$$

where f is the fraction of the scattered energy residing in the forward peak. For the δ-two-stream approximation and δ-two- and four-stream combination approximation, $\ell = 0$, 1 and $f = \tilde{\omega}_2/5$, and for the δ-four-stream approximation, $\ell = 0$, 1, 2, 3 and $f = \tilde{\omega}_4/9$. In the thermal infrared wavelengths, detailed features in the scattering phase function are largely suppressed due to absorption. Thus, we may use the asymmetry factor to represent the phase function through the Henyey–Greenstein function in the form

$$\tilde{\omega}_\ell = (2\ell + 1)g^\ell. \quad (2.27)$$

Use of the δ-function adjustment would enhance the accuracy of approximate treatments of multiple scattering. It should be pointed out that this adjustment has no effect on the absorption approximation.

3. Computational results

In this section, the accuracy of the absorption approximation (AA), the modified δ-two-stream approximation (D2S), the δ-four-stream approximation (D4S), and the δ-two- and four-stream combination approximation (D2/4S) are examined by comparing their results with the ''exact'' values computed from the discrete-ordinates method (Stamnes et al. 1988). In D2S, the value of D is 1.66, and in D2/4S, the value of D is 2. The δ-128-stream (D128S) calculations are used as reference results.

a. Monochromatic emissivity of a single homogeneous layer

We first examine the accuracies of various approximations for the emissivity computation involving a single homogeneous layer with a constant temperature using four pairs of $(\tilde{\omega}, g)$: (0.3637, 0.8487), (0.4982, 0.9467), (0.7105, 0.9044), and (0.7771, 0.7720). The first two are for water clouds at a wavelength of 11 μm with effective radii of $\sim$6 and 15 μm (Hunt 1973). The other two correspond to the conditions for cold cirrus (Ci cold) and altostratus (As) clouds in the spectral interval 1100–1250 cm^{-1} (Fu 1991). Note that the pair (0.4982, 0.9467) is very close to that of cirrostratus (Cs) in the spectral interval 800–980 cm^{-1} (Fu 1991). For each pair of $(\tilde{\omega}, g)$, 11 optical depths ranging from 0.1 to 50 are used in the calculations.

TABLE 1. Comparison of various radiative transfer schemes for the emissivity of a single homogeneous layer with constant temperature. The numbers in parentheses give relative differences (%) between approximate methods and the δ-128-stream scheme (D128S).

Optical depth	D128S	AA	D2S	D4S	D2/4S
		$\bar{\omega} = 0.3637$		$g = 0.8487$	
0.10	0.11286	0.10024 (−11.2)	0.10023 (−11.2)	0.11604 (2.8)	0.11559 (2.4)
0.25	0.24873	0.23208 (−6.7)	0.23197 (−6.7)	0.25558 (2.8)	0.25385 (2.1)
0.50	0.41976	0.41029 (−2.3)	0.40966 (−2.4)	0.42552 (1.4)	0.42245 (0.6)
0.75	0.54515	0.54715 (0.4)	0.54549 (0.1)	0.54648 (0.2)	0.54336 (−0.3)
1.0	0.63963	0.65224 (2.0)	0.64915 (1.5)	0.63701 (−0.4)	0.63458 (−0.8)
2.5	0.89531	0.92868 (3.7)	0.91562 (2.3)	0.89110 (−0.5)	0.89240 (−0.3)
5.0	0.97326	0.99491 (2.2)	0.97522 (0.2)	0.97247 (−0.1)	0.97223 (−0.1)
7.5	0.98271	0.99964 (1.7)	0.97902 (−0.4)	0.98158 (−0.1)	0.98026 (−0.2)
10.0	0.98395	0.99997 (1.6)	0.97927 (−0.5)	0.98260 (−0.1)	0.98105 (−0.3)
25.0	0.98415	1.00000 (1.6)	0.97928 (−0.5)	0.98273 (−0.1)	0.98113 (−0.3)
50.0	0.98415	1.00000 (1.6)	0.97928 (−0.5)	0.98273 (−0.1)	0.98113 (−0.3)
		$\bar{\omega} = 0.4982$		$g = 0.9467$	
0.10	0.09083	0.07992 (−12.0)	0.07992 (−12.0)	0.09327 (2.7)	0.09308 (2.5)
0.25	0.20415	0.18799 (−7.9)	0.18796 (−7.9)	0.21047 (3.1)	0.20965 (2.7)
0.50	0.35354	0.34065 (−3.6)	0.34043 (−3.7)	0.36132 (2.2)	0.35965 (1.7)
0.75	0.46905	0.46460 (−0.9)	0.46402 (−1.1)	0.47432 (1.1)	0.47236 (0.7)
1.0	0.56052	0.56525 (0.8)	0.56411 (0.6)	0.56220 (0.3)	0.56039 (0.0)
2.5	0.84356	0.87538 (3.8)	0.86929 (3.1)	0.83774 (−0.7)	0.83846 (−0.6)
5.0	0.96203	0.98447 (2.3)	0.97319 (1.2)	0.96093 (−0.1)	0.96170 (0.0)
7.5	0.98440	0.99806 (1.4)	0.98548 (0.1)	0.98387 (−0.1)	0.98362 (−0.1)
10.0	0.98810	0.99976 (1.1)	0.98693 (−0.2)	0.98815 (−0.1)	0.98747 (−0.2)
25.0	0.99026	1.00000 (1.0)	0.98712 (−0.3)	0.98913 (−0.1)	0.98827 (−0.2)
50.0	0.99026	1.00000 (1.0)	0.98712 (−0.3)	0.98913 (−0.1)	0.98827 (−0.2)
		$\bar{\omega} = 0.7105$		$g = 0.9044$	
0.10	0.05455	0.04692 (−14.0)	0.04692 (−14.0)	0.05547 (1.7)	0.05516 (1.1)
0.25	0.12755	0.11321 (−11.2)	0.11318 (−11.3)	0.13031 (2.2)	0.12881 (1.0)
0.50	0.23216	0.21360 (−8.0)	0.21338 (−8.1)	0.23646 (1.9)	0.23252 (0.2)
0.75	0.32056	0.30262 (−5.6)	0.30198 (−5.8)	0.32435 (1.2)	0.31850 (−0.6)
1.0	0.39629	0.38157 (−3.7)	0.38022 (−4.1)	0.39840 (0.5)	0.39146 (−1.2)
2.5	0.68407	0.69923 (2.2)	0.68852 (0.6)	0.67749 (−1.0)	0.67423 (−1.4)
5.0	0.86918	0.90954 (4.6)	0.87857 (1.1)	0.86491 (−0.5)	0.86775 (−0.2)
7.5	0.92833	0.97279 (4.8)	0.92924 (0.1)	0.92619 (−0.2)	0.92754 (−0.1)
10.0	0.94816	0.99182 (4.6)	0.94262 (−0.6)	0.94625 (−0.2)	0.94507 (−0.3)
25.0	0.95856	0.99999 (4.3)	0.94740 (−1.2)	0.95598 (−0.3)	0.95196 (−0.7)
50.0	0.95858	1.00000 (4.3)	0.94740 (−1.2)	0.95599 (−0.3)	0.95196 (−0.7)
		$\bar{\omega} = 0.7771$		$g = 0.7720$	
0.10	0.04264	0.03633 (−14.8)	0.03632 (−14.8)	0.04312 (1.1)	0.04253 (−0.3)
0.25	0.10132	0.08835 (−12.8)	0.08831 (−12.8)	0.10264 (1.3)	0.09977 (−1.5)
0.50	0.18827	0.16890 (−10.3)	0.16856 (−10.5)	0.18991 (0.9)	0.18225 (−3.2)
0.75	0.26423	0.24233 (−8.3)	0.24127 (−8.7)	0.26499 (0.3)	0.25338 (−4.1)
1.0	0.33108	0.30927 (−6.6)	0.30697 (−7.3)	0.33044 (−0.2)	0.31640 (−4.4)
2.5	0.60040	0.60348 (0.5)	0.58279 (−2.9)	0.59507 (−0.9)	0.58680 (−2.3)
5.0	0.78721	0.84277 (7.1)	0.77377 (−1.7)	0.78411 (−0.4)	0.78637 (−0.1)
7.5	0.84888	0.93766 (10.5)	0.83121 (−2.1)	0.84675 (−0.3)	0.84543 (−0.4)
10.0	0.86943	0.97528 (12.2)	0.84803 (−2.5)	0.86721 (−0.3)	0.86116 (−1.0)
25.0	0.87974	0.99990 (13.7)	0.85491 (−2.8)	0.87705 (−0.3)	0.86641 (−1.5)
50.0	0.87975	1.00000 (13.7)	0.85491 (−2.8)	0.87706 (−0.3)	0.86641 (−1.5)

For a homogeneous layer without incident radiation, the emissivity is defined as

$$\varepsilon = F/\pi B(T), \tag{3.1}$$

where F is the radiative flux emerging from the surface of the layer and $B(T)$ is the Planck function of the layer. Table 1 shows the emissivity results; the numbers in parentheses give the relative differences between the approximate and exact schemes.

For small optical depths ($\tau_1 < \sim 0.25$), the relative errors in emissivity for AA and D2S are larger than 10%. This is because the exact diffusivity factor is not a constant of 1.66 but increases with decreasing optical depth. When $\tau_1 \to 0$, it has a value of 2. The errors of AA are also large when the scattering effect becomes significant. For a single-scattering albedo and asymmetry factor of (0.7771, 0.7720), the relative errors can be as large as 13.7% for large optical depths. These errors, however, are reduced to 2.8% in the case of D2S, in which multiple scattering effects are included. For D4S, the emissivity has an accuracy within ~3%. The accuracy of D2/4S is very close to that of D4S. The

TABLE 2. Comparison of various radiative transfer schemes for the effective downward emissivity of a homogeneous layer with isotropic incident radiation at the bottom. The numbers in parentheses give relative differences (%) between approximate methods and the δ-128-stream scheme.

Optical depth	D128S	AA	D2S	D4S	D2/4S
		$\bar{\omega} = 0.7105$	$g = 0.9044$	$F^{\uparrow}(\tau_1) = 5\pi B(T)$	
0.10	0.09828	0.04692 (−52.3)	0.07365 (−25.1)	0.10055 (2.3)	0.08640 (−12.1)
0.25	0.21013	0.11321 (−46.1)	0.17499 (−16.7)	0.22285 (6.1)	0.19826 (−5.7)
0.50	0.35412	0.21360 (−39.7)	0.32248 (−8.9)	0.37615 (6.2)	0.34885 (−1.5)
0.75	0.46685	0.30262 (−35.2)	0.44724 (−4.2)	0.49019 (5.0)	0.46748 (0.1)
1.0	0.55885	0.38157 (−31.7)	0.55316 (−1.0)	0.57994 (3.8)	0.56378 (0.9)
2.5	0.88241	0.69923 (−20.8)	0.93359 (5.8)	0.88952 (0.8)	0.90185 (2.2)
5.0	1.07545	0.90954 (−15.4)	1.14057 (6.1)	1.08411 (0.8)	1.10719 (3.0)
7.5	1.13533	0.97279 (−14.3)	1.19241 (5.0)	1.14613 (1.0)	1.16770 (2.9)
10.0	1.15525	0.99182 (−14.1)	1.20587 (4.4)	1.16627 (1.0)	1.18528 (2.6)
25.0	1.16565	0.99999 (−14.2)	1.21065 (3.9)	1.17601 (0.9)	1.19217 (2.3)
50.0	1.16567	1.00000 (−14.2)	1.21066 (3.9)	1.17602 (0.9)	1.19217 (2.3)
		$\bar{\omega} = 0.7105$	$g = 0.9044$	$F^{\uparrow}(\tau_1) = 2.5\pi B(T)$	
0.10	0.07642	0.04692 (−38.6)	0.06028 (−21.1)	0.07801 (2.1)	0.07078 (−7.4)
0.25	0.16884	0.11321 (−32.9)	0.14408 (−14.7)	0.17658 (4.6)	0.16353 (−3.1)
0.50	0.29314	0.21360 (−27.1)	0.26793 (−8.6)	0.30630 (4.5)	0.29069 (−0.8)
0.75	0.39371	0.30262 (−23.1)	0.37461 (−4.9)	0.40727 (3.4)	0.39299 (−0.2)
1.0	0.47757	0.38157 (−20.1)	0.46669 (−2.3)	0.48917 (2.4)	0.47762 (0.0)
2.5	0.78324	0.69923 (−10.7)	0.81105 (3.6)	0.78351 (0.0)	0.78804 (0.6)
5.0	0.97232	0.90954 (−6.5)	1.00957 (3.8)	0.97451 (0.2)	0.98747 (1.6)
7.5	1.03183	0.97279 (−5.7)	1.06082 (2.8)	1.03616 (0.4)	1.04762 (1.5)
10.0	1.05171	0.99182 (−5.7)	1.07424 (2.1)	1.05626 (0.4)	1.06517 (1.3)
25.0	1.06211	0.99999 (−5.8)	1.07903 (1.6)	1.06600 (0.4)	1.07206 (0.9)
50.0	1.06213	1.00000 (−5.8)	1.07903 (1.6)	1.06601 (0.4)	1.07207 (0.9)
		$\bar{\omega} = 0.7771$	$g = 0.7720$	$F^{\uparrow}(\tau_1) = 2\pi B(T)$	
0.10	0.08294	0.03633 (−56.2)	0.06427 (−22.5)	0.08614 (3.9)	0.07505 (−9.5)
0.25	0.18164	0.08835 (−51.4)	0.15313 (−15.7)	0.19134 (5.3)	0.17200 (−5.3)
0.50	0.31273	0.16890 (−46.0)	0.28356 (−9.3)	0.32618 (4.3)	0.30370 (−2.9)
0.75	0.41809	0.24233 (−42.0)	0.39517 (−5.5)	0.43024 (2.9)	0.41007 (−1.9)
1.0	0.50577	0.30927 (−38.9)	0.49109 (−2.9)	0.51505 (1.8)	0.49916 (−1.3)
2.5	0.82609	0.60348 (−26.9)	0.84937 (2.8)	0.82620 (0.0)	0.83677 (1.3)
5.0	1.02611	0.84277 (−17.9)	1.06224 (3.5)	1.02845 (0.2)	1.05244 (2.6)
7.5	1.08921	0.93766 (−13.9)	1.12151 (3.0)	1.09247 (0.3)	1.11255 (2.1)
10.0	1.10991	0.97528 (−12.1)	1.13848 (2.6)	1.11308 (0.3)	1.12834 (1.7)
25.0	1.12023	0.99990 (−10.7)	1.14537 (2.2)	1.12293 (0.2)	1.13359 (1.2)
50.0	1.12025	1.00000 (−10.7)	1.14538 (2.2)	1.12294 (0.2)	1.13359 (1.2)

results displayed in Table 1 suggest that the scattering effects in the infrared radiative transfer can be properly treated by using D2S, whereas two double Gauss quadrature points are sufficient to determine the flux from the intensity distribution.

By assuming no downward flux at the top of the cloud layer, the effective downward emissivity is defined by

$$\varepsilon^{\downarrow} = F^{\downarrow}(\tau_1)/\pi B(T), \tag{3.2}$$

where $F^{\downarrow}(\tau_1)$ is the downward flux at the bottom of the layer. Table 2 lists the effective downward emissivity for two pairs of single-scattering albedo and asymmetry factor with different isotropic radiation incident from the bottom. The relative differences between approximate and reference results are given in parentheses. The effective emissivity can be as large as 1.2 because of the multiple scattering effect. For small optical depths where more than half of the effective emissivity is due to the scattering, the relative errors for AA can be larger than 50%. The maximum errors in the effective emissivity for D2S, D4S, and D2/4S are ~25%, ~6%, and ~12%, respectively. For $\tau_1 > \sim 0.1$, D4S and D2/4S have accuracies within ~6%.

Note that AA in Table 2 has identical values for effective downward emissivity in the cases with incident radiation of $5\pi B(T)$ and $2.5\pi B(T)$. The effective downward emissivity with D128S does indeed vary with the incident radiation. A scheme that accounts for the thermal infrared scattering by treating effective emissivity as an intrinsic property of a cloud is thus limited (because the effective emissivity depends on the radiative environment as well as on the cloud).

b. Broadband atmospheric radiative heating rates and fluxes

For GCM and remote sensing applications, it is important to evaluate errors produced by radiative transfer approximations in the calculation of heating rates and fluxes under a variety of atmospheric conditions. In the infrared spectrum (0–2200 cm^{-1}), the nongray gaseous absorption due to H_2O, CO_2, O_3, CH_4, and N_2O is in-

TABLE 3. Comparison of various radiative transfer schemes for infrared fluxes (W m^{-2}) at the top and surface using the midlatitude summer atmosphere. The numbers in parentheses give differences (W m^{-2}) between approximate methods and the δ-128-stream scheme.

Atmospheric conditions	D128S	AA	D2S	D4S	D2/4S
			$F\uparrow$(TOA)		
Clear sky	283.7	283.7 (0.0)	283.8 (0.1)	283.3 (−0.4)	283.3 (−0.4)
Low cloud	266.0	271.2 (5.2)	264.1 (−1.9)	265.8 (−0.2)	264.8 (−1.2)
Middle cloud	229.6	236.0 (6.4)	227.8 (−1.8)	229.4 (−0.2)	228.5 (−1.1)
High cloud	215.6	221.6 (6.0)	214.1 (−1.5)	214.9 (−0.7)	215.4 (−0.2)
Low, middle, and high clouds	188.0	196.2 (8.2)	186.2 (−1.8)	187.6 (−0.4)	187.2 (−0.8)
			$F\downarrow$(SFC)		
Clear sky	347.4	348.0 (0.6)	348.0 (0.6)	348.2 (0.8)	348.2 (0.8)
Low cloud	412.1	411.5 (−0.6)	412.2 (0.1)	412.0 (−0.1)	412.1 (0.0)
Middle cloud	393.6	392.3 (−1.3)	394.2 (0.6)	393.8 (0.2)	394.1 (0.5)
High cloud	355.1	355.6 (0.5)	356.6 (1.5)	355.6 (0.5)	355.8 (0.7)
Low, middle, and high clouds	412.1	411.5 (−0.6)	412.2 (0.1)	412.0 (−0.1)	412.1 (0.0)

corporated into multiple scattering models based on the correlated k-distribution method developed by Fu and Liou (1992). The continuum absorption of H_2O is included in the spectral region 280–1250 cm^{-1}. For ice clouds, the single-scattering properties are parameterized in terms of ice water content (IWC) and mean effective size (D_e) (Fu and Liou 1993). The single-scattering properties of water clouds are parameterized in terms of liquid water content (LWC) and effective radius (r_e) (Fu 1991).

Two atmospheric profiles, including the midlatitude summer (MLS) and subarctic winter (SAW) of McClatchey et al. (1971), are used in the flux and heating rate calculations. The CO_2, CH_4, and N_2O mixing ratios are assumed to be uniform throughout the atmosphere with concentrations of 330, 1.6, and 0.28 ppmv, respectively. For each profile, five calculations are performed: clear sky; skies with low cloud (LWC = 0.22 g m^{-3}, r_e = 5.89 μm); skies with middle cloud (LWC = 0.28 g m^{-3}, r_e = 6.2 μm); skies with high cloud (IWC = 0.0048 g m^{-3}, D_e = 41.5 μm); and skies with all three clouds. The visible optical depths for low, middle, and high clouds are ~60, ~72, and ~0.8, respectively. The low cloud is positioned from 1.0 to 2.0 km in MLS and from 0.5 to 1.5 km in SAW, while the middle cloud extends from 4.0 to 5.0 km in MLS, and from 2.0 to 3.0 km in SAW. The high cloud is located between 10 and 12 km in MLS and between 6 and 8 km in SAW. In the calculations, the atmosphere is equally divided into numerous homogeneous layers with a vertical resolution of 0.25 km and the surface emissivity is set to one.

Comparisons of the upward flux at the top of the atmosphere (TOA) and the downward flux at the surface between various radiative transfer approximations and D128S are shown in Tables 3 and 4 for MLS and SAW, respectively. Under clear-sky conditions, the D2S and D4S methods reduce to the AA and D2/4S methods, respectively. The numerical values in Tables 3 and 4 for AA and D2/4S with clear skies differ slightly; for AA (D2/4S) we used a D of 1.66 (2.00). The errors in fluxes with clear skies computed from various radiative transfer parameterizations are less than 1 W m^{-2}. In cloudy conditions, the AA method consistently overestimates the TOA fluxes by ~5–8 W m^{-2}. This is because the AA method overestimates emissivity for optically thick

TABLE 4. Same as in Table 3 except for the subarctic winter atmosphere.

Atmospheric conditions	D128S	AA	D2S	D4S	D2/4S
			$F\uparrow$(TOA)		
Clear sky	200.7	200.8 (0.1)	200.8 (0.1)	200.4 (−0.3)	200.4 (−0.3)
Low cloud	196.9	201.3 (4.4)	195.4 (−1.5)	196.6 (−0.3)	195.9 (−1.0)
Middle cloud	188.2	193.0 (4.8)	186.7 (−1.5)	187.9 (−0.3)	187.1 (−1.1)
High cloud	169.5	173.9 (4.4)	168.7 (−0.8)	168.8 (−0.7)	169.0 (−0.5)
Low, middle, and high clouds	163.9	169.8 (5.9)	162.3 (−1.6)	163.4 (−0.5)	163.0 (−0.9)
			$F\downarrow$(SFC)		
Clear sky	168.6	169.4 (0.8)	169.4 (0.8)	168.9 (0.3)	168.9 (0.3)
Low cloud	249.1	249.2 (0.1)	249.0 (−0.1)	249.0 (−0.1)	249.0 (−0.1)
Middle cloud	245.3	245.1 (−0.2)	245.3 (0.0)	245.2 (−0.1)	245.3 (0.0)
High cloud	188.7	188.4 (−0.3)	190.1 (1.4)	188.9 (0.2)	188.9 (0.2)
Low, middle, and high clouds	249.1	249.2 (0.1)	249.0 (−0.1)	249.0 (−0.1)	249.0 (−0.1)

clouds and tends to underestimate it for optically thin clouds (Table 1). The error associated with AA is significant in climate studies. It should be noted that the TOA fluxes are only reduced by $\sim$4 W m^{-2} due to the doubling of CO_2 concentration. The downward surface fluxes using AA agree with those computed from D128S within $\sim$1 W m^{-2}. For D2S, D4S, and D2/4S, Tables 3 and 4 show that the maximum errors in fluxes are 1.9, 0.8, and 1.2 W m^{-2}, respectively.

Figures 1–5 show the comparison of heating rates in clear sky; skies with low, middle, high cloud; and a combination of all three. The heating rate profiles calculated from the D128S method are shown in panels (a) and (c) of each figure, while the corresponding error profiles for the results computed from AA, D2S, D4S, and D2/4S are shown in panels (b) and (d). In each figure, (a) and (b) are for MLS and (c) and (d) are for SAW. It can be seen that errors in the heating rates in SAW are smaller than those in MLS. For clear sky, errors in the heating rates are less than 0.1 K day^{-1} using AA and D2S, and less than 0.03 K day^{-1} using D4S and D2/4S, as shown in Fig. 1. For cloudy skies, as shown in Figs. 2–5, the maximum errors in heating rates, which occur near the cloud tops, are 3.9, 1.5, 0.4, and 0.7 K day^{-1} for AA, D2S, D4S, and D2/4S, respectively. The second maximum in errors occurs near the cloud bases. It is noted that AA overestimates the heating rates above low and middle cloud tops and underestimates them below the high cloud base. Recall that AA showed the largest errors for outgoing longwave radiation (OLR) with clouds. For the atmosphere containing high cloud, relative errors in the heating rates within clouds can reach more than 30% for both AA and D2S (Figs. 4 and 5).

Finally, Table 5 shows infrared fluxes at the top and surface of MLS determined from the δ-128-stream scheme, δ-Eddington, δ-hemispheric mean two-stream, and δ-discrete-ordinates two-stream approximations. The δ-Eddington and δ-hemispheric mean two-stream schemes can produce errors greater than 10 W m^{-2}, whereas the δ-discrete-ordinates two-stream approximation overestimates the fluxes by $\sim$25–60 W m^{-2}. We see that none of the conventional two-stream approximations produces results better than those from the simple absorption approximation! From these comparisons, it is clear that proper modifications to conventional two-stream approximations are needed for applications to infrared radiative transfer.

4. Discussion

For applications to three-dimensional dynamic models and satellite remote sensing of the radiative budget on a global scale, rapid computations of the radiative fluxes and heating rates are required. Thus, it is important to examine not only the accuracy but also the efficiency of radiative transfer parameterizations. Table 6 presents the computer time comparisons for broadband heating rate and flux calculations using various radiative transfer approximations. For these comparisons, the atmosphere is divided into 100 layers and the computing time is normalized to that of D2S. The first line shows the computer time used by the radiative transfer modules only, whereas the second line gives the total computer time required for the complete heating rate and flux calculations. The overhead calculations to prepare the single-scattering properties of the layers and the Planck function would reduce the differences in radiation model efficiency produced from different transfer modules. Although the computing time spent on overhead calculations can be model dependent, the timing shown for the transfer module should be universal (the optimization of codes may result in $\sim$10% differences).

The AA method is most computationally efficient for infrared radiative transfer calculations. However, as demonstrated in section 3, this approximation produces significant errors in fluxes and heating rates under cloudy conditions. In the Fu–Liou radiation model (Fu and Liou 1992, 1993), the use of AA instead of D4S is only $\sim$20% faster than the model employing D2S. Therefore, the advantage in using AA appears quite limited.

High accuracy in radiative fluxes and heating rates can be obtained by using D4S. The D4S radiation scheme (Fu and Liou 1992, 1993) has been incorporated into two-dimensional cloud dynamic models to study cloud–radiation interactions in different cloud systems: tropical deep convection systems (Fu et al. 1995; Chin et al. 1995) and a subtropical marine boundary cloud system (Krueger et al. 1995a,b). Charlock and Alberta (1996) applied Fu and Liou's model in the CERES/ARM/GEWEX experiment to study the surface and atmospheric radiative energy budget over the ARM SGP CART site in Oklahoma. Although the D4S method is most accurate, the computer time requirement associated with it is substantial compared to the other three methods.

The D2S method is sufficiently economical for infrared radiative transfer calculations, and under most atmospheric conditions, it produces reasonable accuracy. Therefore, this method can be very useful in many applications. However, it should be noted that large errors can be generated when the optical depth is small (see Tables 1 and 2), and for this reason D2S may not be a good approximation for an atmosphere containing cirrus clouds (see Figs. 4 and 5). In addition, an error of $\sim$2 W m^{-2} in the upward flux at the top of the atmosphere (Tables 3 and 4) could be significant in some climate studies.

As shown in section 3, the accuracy of D2/4S is close to that of D4S, which is reliable under all atmospheric conditions. The computational time of D2/4S is about four times faster than that of D4S and only 50% more than that of D2S (Table 6). In view of the overall high accuracy and computational economy, it appears that the D2/4S method is well suited for flux and heating

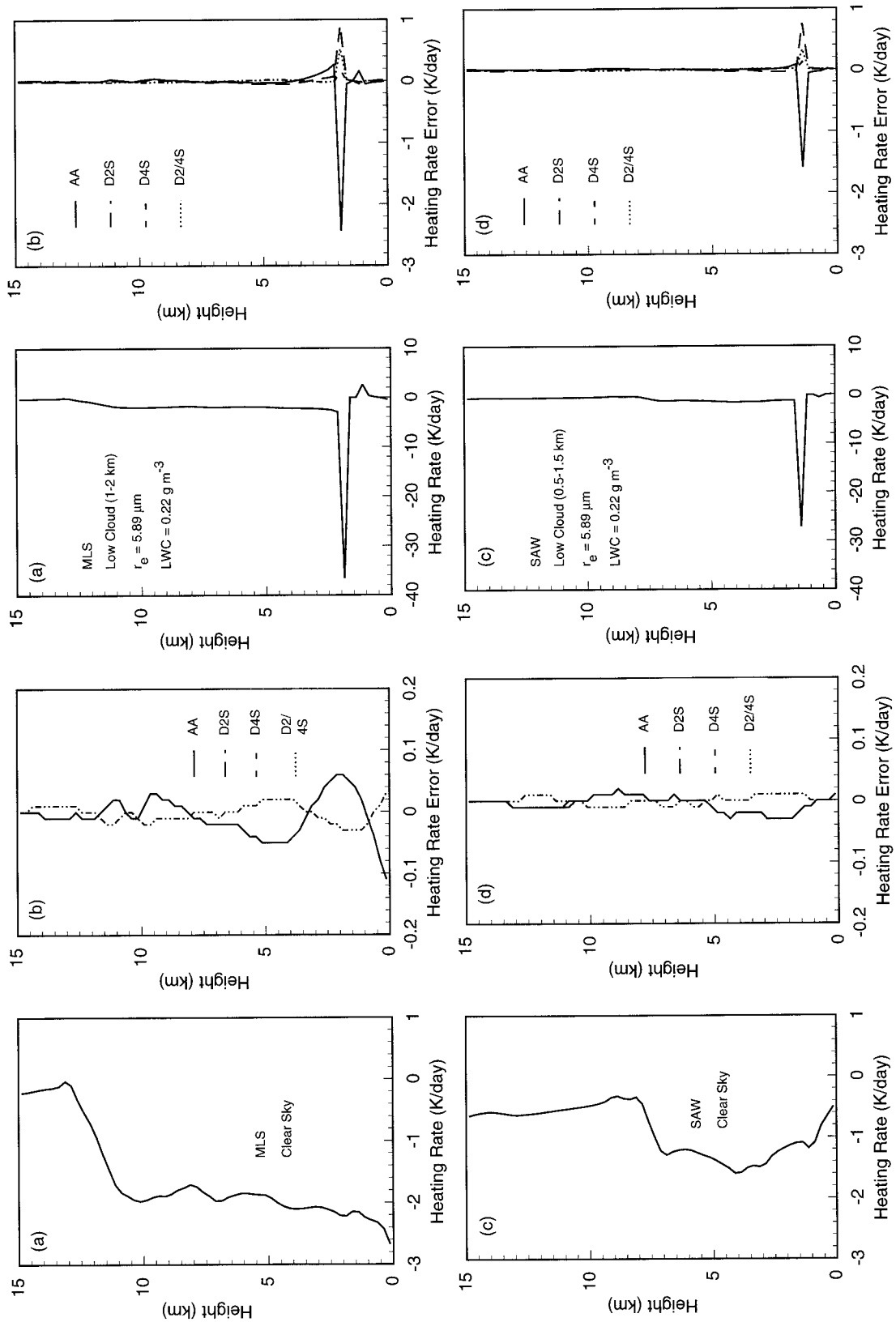

FIG. 1. Infrared heating rate profiles computed from the δ-128-stream scheme and the error profiles produced by various radiative transfer approximations in the clear sky. (a) and (b): The midlatitude summer atmosphere (MLS); (c) and (d): the subarctic winter atmosphere (SAW). Under clear-sky conditions, the results from D2S and D4S reduce to those from AA and D2/4S, respectively.

FIG. 2. As in Fig. 1 except for the sky containing low cloud.

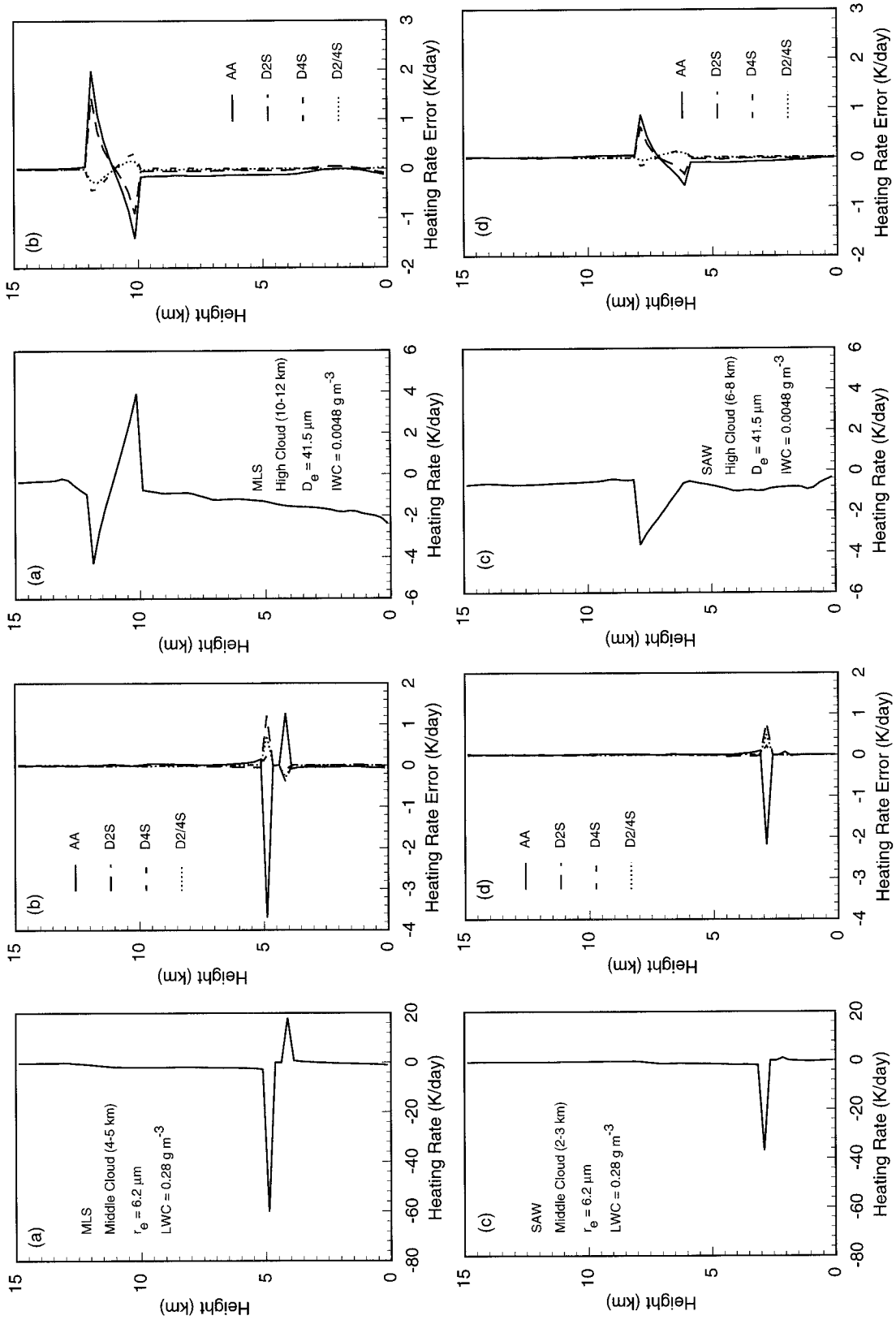

FIG. 3. As in Fig. 1 except for the sky containing middle cloud.

FIG. 4. As in Fig. 1 except for the sky containing high cloud.

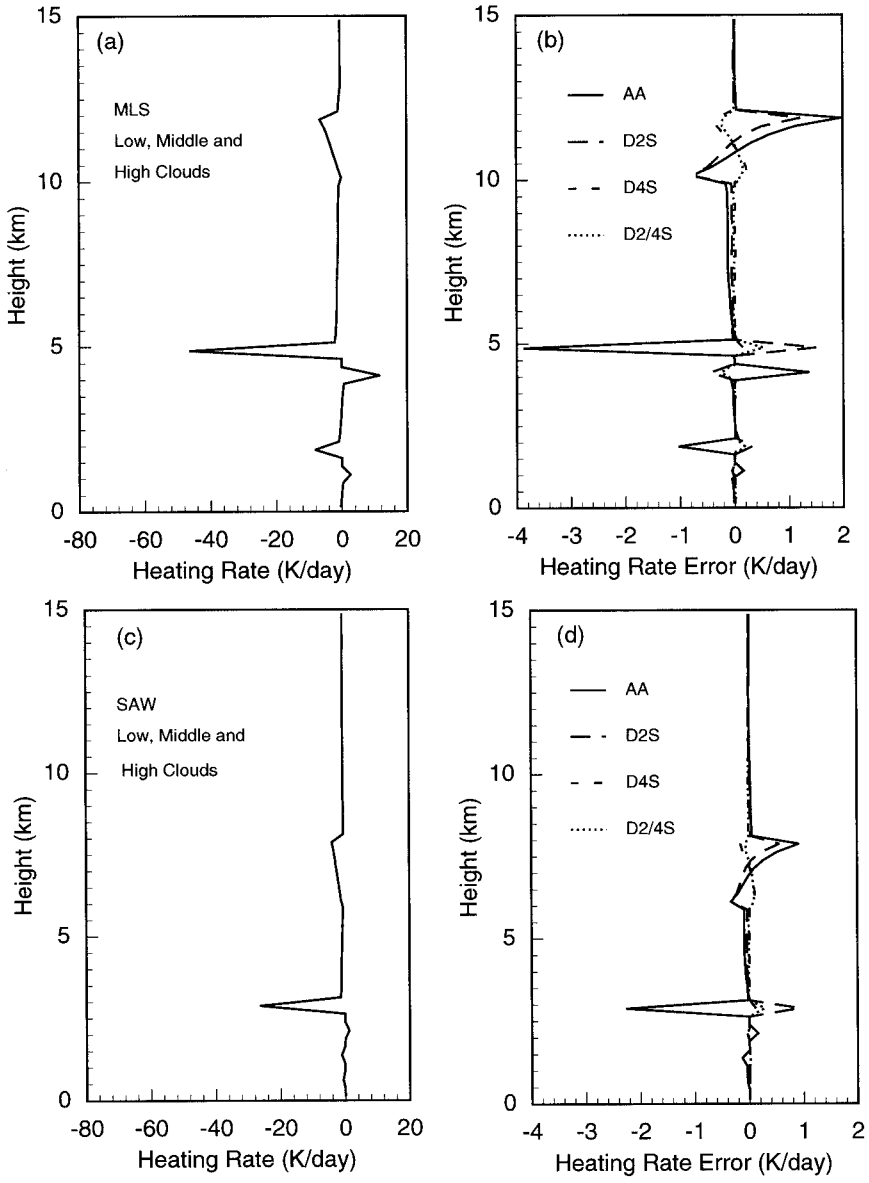

FIG. 5. As in Fig. 1 except for the sky containing low, middle, and high clouds.

rate calculations in GCM and satellite remote sensing applications.

5. Summary and conclusions

In this paper, we have presented a systematic formulation of various radiative transfer approximations for infrared flux calculations in a consistent manner. In the absorption approximation, a diffusivity factor of 1.66 is used. We have introduced a modified two-stream scheme, which is consistent with the absorption approximation in the limit of no scattering. In the four-stream scheme and two- and four-stream combination scheme, the double Gauss quadrature is used, which provides the correct relation between flux and intensity from an isotropic source. In all radiative transfer parameterizations, we express the Planck function as an exponential function of optical depth.

A wide range of accuracy checks are performed for various radiative transfer parameterizations in the calculation of the monochromatic emissivity for a homogeneous layer as well as broadband heating rates and fluxes in nonhomogeneous atmospheres. We find that the scattering processes cannot be neglected in the computation of infrared radiative transfer under cloudy conditions. The modified δ-two-stream scheme can yield acceptable results under most atmospheric conditions. However, errors can become substantial when the optical depth is small, particularly in cirrus cloud conditions. For the δ-four-stream scheme, reliable results are

TABLE 5. Comparison of conventional two-stream parameterizations and the δ-128-stream scheme for infrared fluxes (W m^{-2}) at the top and surface using the midlatitude summer atmosphere. The numbers in parentheses give differences (W m^{-2}) between approximate methods and the δ-128-stream scheme.

Atmospheric conditions	D128S	δ-Eddington	δ-hemispheric mean two-stream	δ-discrete ordinates two-stream
		$F\uparrow$(TOA)		
Clear sky	283.7	300.4 (16.7)	278.5 (−5.2)	317.0 (33.3)
Low cloud	266.0	282.5 (16.5)	260.4 (−5.6)	303.8 (37.8)
Middle cloud	229.6	244.1 (14.5)	225.7 (−3.9)	262.3 (32.7)
High cloud	215.6	225.9 (10.3)	202.4 (−13.2)	239.4 (23.8)
Low, middle, and high clouds	188.0	198.4 (10.4)	179.5 (−8.5)	213.1 (25.1)
		$F\downarrow$(SFC)		
Clear sky	347.4	348.9 (1.5)	356.4 (9.0)	404.0 (56.6)
Low cloud	412.1	411.7 (−0.4)	412.6 (0.5)	475.1 (63.0)
Middle cloud	393.6	392.8 (−0.8)	396.5 (2.9)	455.3 (61.7)
High cloud	355.1	355.3 (0.2)	364.8 (9.7)	413.8 (58.7)
Low, middle, and high clouds	412.1	411.7 (−0.4)	412.6 (0.5)	475.1 (63.0)

obtained under all atmospheric conditions. The accuracy of the δ-two- and four-stream combination scheme is close to that of the δ-four-stream scheme. We further illustrate that conventional two-stream schemes are not appropriate for applications to infrared radiative transfer.

The computational efficiency for various radiative transfer approximations is compared. The results presented in this paper on the accuracy and efficiency for various radiative transfer parameterizations can be utilized to determine which approximate method is most appropriate for a particular application. In view of its overall high accuracy and computational economy, the δ-two- and four-stream combination technique appears to be well suited for typical GCM applications associated with weather and climate studies.

Acknowledgments. The research work contained herein has been supported by NSERC Operating Grant, AES Science Subvention Grant, NSERC Collaborative Grant, NASA Grant NAG1-1719, and in part by DOE Grant DE-FG02-97ER62363.

TABLE 6. Timing of infrared heating rate and flux calculations using various radiative transfer approximations (normalized to the computing time of the D2S method).

	AA	D2S	D4S	D2/4S
Radiative transfer module only	0.25	1.0	9.0	1.8
Radiation model*	0.83	1.0	5.2	1.5

* The nongray gaseous absorption is treated by using the correlated k-distribution method (Fu and Liou 1992). The parameterization of the single-scattering properties of cloud particles follows Fu and Liou (1993) and Fu (1991).

APPENDIX

Discretization of the Radiative Transfer Equation

In the context of the discrete-ordinates method for radiative transfer (Liou 1992), we may first expand the scattering phase function in terms of Legendre polynomials P_ℓ in the form

$$P(\cos\Theta) = \sum_{\ell=0}^{N} \tilde{\omega}_\ell P_\ell(\cos\Theta), \tag{A.1}$$

where the moments $\tilde{\omega}_\ell$ can be determined from the orthogonal property of Legendre polynomials as follows:

$$\tilde{\omega}_\ell = \frac{2\ell + 1}{2} \int_{-1}^{1} P(\cos\Theta) P_\ell(\cos\Theta)\, d\cos\Theta. \tag{A.2}$$

In our notation, $\tilde{\omega}_0 = 1$, and $\tilde{\omega}_1/3 = g$, the asymmetry factor.

Using the additional theorem for Legendre polynomials, the azimuth-independent phase function may be written as

$$P(\mu, \mu') = \sum_{l=0}^{N} \tilde{\omega}_l P_l(\mu) P_l(\mu'). \tag{A.3}$$

Replacing the integral by summation, according to the Gauss quadrature, and using the phase function expansion expression in Eq. (A.3), we obtain the discrete-ordinates approximation for Eq. (2.1) in the form

$$\mu_i \frac{dI(\tau, \mu_i)}{d\tau} = I(\tau, \mu_i) - \frac{\tilde{\omega}}{2} \sum_{\ell=0}^{N} \tilde{\omega}_\ell P_\ell(\mu_i) \times \sum_{j=-n}^{n} I(\tau, \mu_j) P_\ell(\mu_j) a_j - (1 - \tilde{\omega}) B(T), \quad i = \pm 1, \ldots, \pm n, \tag{A.4}$$

where the quadrature point $\mu_{-j} = -\mu_j$, $j \neq 0$, and the

weight $a_{-j} = a_j$ and $\Sigma_{j=-n}^{n} a_j = 2$. The upward and downward fluxes at a given level τ are then defined by

$$F^{\pm}(\tau) = 2\pi \sum_{i=1}^{n} a_i \mu_i I(\tau, \pm\mu_i). \qquad \text{(A.5)}$$

REFERENCES

Charlock, T. P., and T. L. Alberta, 1996: The CERES/ARM/GEWEX experiment (CAGEX) for the retrieval of radiative fluxes with satellite data. *Bull. Amer. Meteor. Soc.,* **77,** 2673–2683.

Chin, H. N. S., Q. Fu, M. M. Bradley, and C. R. Molenkamp, 1995: Modeling of a tropical squall line in two dimensions: Sensitivity to radiation and comparison with a midlatitude case. *J. Atmos. Sci.,* **52,** 3172–3193.

Cuzzi, J. N., T. P. Ackerman, and L. C. Helmle, 1982: The delta-four-stream approximation for radiative transfer. *J. Atmos. Sci.,* **39,** 917–925.

Fouquart, Y., J. C. Buriez, M. Herman, and R. S. Kandel, 1990: The influence of clouds on radiation: A climate-modeling perspective. *Rev. Geophys.,* **28,** 145–166.

Fu, Q., 1991: Parameterization of radiative processes in vertically nonhomogeneous multiple scattering atmospheres. Ph.D. dissertation, University of Utah, 259 pp. [Available from University Microfilm, 305 N. Zeeb Rd., Ann Arbor, MI 48106.]

——, and K. N. Liou, 1992: On the correlated k-distribution method for radiative transfer in nonhomogeneous atmospheres. *J. Atmos. Sci.,* **49,** 2139–2156.

——, and ——, 1993: Parameterization of the radiative properties of cirrus clouds. *J. Atmos. Sci.,* **50,** 2008–2025.

——, S. K. Krueger, and K. N. Liou, 1995: Interactions between radiation and convection in simulated tropical cloud clusters. *J. Atmos. Sci.,* **52,** 1310–1328.

Goody, R. M., 1964: *Theoretical Basis.* Vol. I, *Atmospheric Radiation,* Oxford University Press, 519 pp.

Hunt, G. E., 1973: Radiative properties of terrestrial clouds at visible and infrared thermal window wavelengths. *Quart. J. Roy. Meteor. Soc.,* **99,** 346–369.

Joseph, J. H., W. J. Wiscombe, and J. A. Weinman, 1976: The delta-Eddington approximation for radiative transfer. *J. Atmos. Sci.,* **33,** 2452–2459.

King, M. D., and Harshvardhan, 1986: Comparative accuracy of selected multiple scattering approximations. *J. Atmos. Sci.,* **43,** 784–801.

Krueger, S. K., G. T. McLean, and Q. Fu, 1995a: Numerical simulation of the stratus to cumulus transition in the subtropical marine boundary layer. Part I: Boundary layer structure. *J. Atmos. Sci.,* **52,** 2839–2850.

——, ——, and ——, 1995b: Numerical simulation of the stratus to cumulus transition in the subtropical marine boundary layer. Part II: Boundary layer circulation. *J. Atmos. Sci.,* **52,** 2851–2868.

Kylling, A., and K. Stamnes, 1992: Efficient yet accurate solution of the linear transport equation in the presence of internal sources: The exponential-linear-in-depth approximation. *J. Comput. Phys.,* **102,** 265–276.

——, ——, and S. C. Tsay, 1995: A reliable and efficient two-stream algorithm for spherical radiative transfer: Documentation of accuracy in realistic layered media. *J. Atmos. Chem.,* **21,** 115–150.

Liou, K. N., 1974: Analytic two-stream and four-stream solutions for radiative transfer. *J. Atmos. Sci.,* **31,** 1473–1475.

——, 1986: Influence of cirrus clouds on weather and climate processes: A global perspective. *Mon. Wea. Rev.,* **114,** 1167–1199.

——, 1992: *Radiative and Cloud Processes in the Atmosphere: Theory, Observation, and Parameterization.* Oxford University Press, 487 pp.

——, Q. Fu, and T. P. Ackerman, 1988: A simple formulation of the delta-four-stream approximation for radiative transfer parameterizations. *J. Atmos. Sci.,* **45,** 1940–1947.

McClatchey, R. A., R. W. Fenn, J. E. A. Selby, F. E. Volz, and J. S. Garing, 1971: Optical properties of the atmosphere. Air Force Rep. AFCRL-71-0279, 85 pp. [Available from Air Force Geophysics Laboratory Lab., Bedford, MA 01731.]

Meador, W. E., and W. R. Weaver, 1980: Two-stream approximation to radiative transfer in planetary atmospheres: A unified description of existing methods and new improvement. *J. Atmos. Sci.,* **37,** 1279–1290.

Prabhakara, C., and G. Dalu, 1976: Remote sensing of the surface emissivity at 9 μm over the globe. *J. Geophys. Res.,* **81,** 3719–3724.

Ritter, B., and J. F. Geleyn, 1992: A comprehensive radiation scheme for numerical weather prediction models with potential applications in climate simulations. *Mon. Wea. Rev.,* **120,** 303–325.

Salisbury, J., and D. D'Aria, 1992: Emissivity of terrestrial materials in the 8–14 μm atmospheric window. *Remote Sens. Environ.,* **42,** 83–106.

Shibata, K., and A. Uchiyama, 1992: Accuracy of the delta-four-stream approximation in inhomogeneous scattering atmospheres. *J. Meteor. Soc. Japan,* **70,** 1097–1109.

Smith, W. L., and Coauthors, 1996: Observations of the infrared radiative properties of the ocean—Implications for the measurement of sea surface temperature via satellite remote sensing. *Bull. Amer. Meteor. Soc.,* **77,** 41–51.

Stackhouse, P. W., Jr., and G. L. Stephens, 1991: A theoretical and observational study of the radiative properties of cirrus: Results from FIRE 1986. *J. Atmos. Sci.,* **48,** 2044–2059.

Stamnes, K., S. Tsay, W. Wiscombe, and K. Jayaweera, 1988: Numerically stable algorithm for discrete-ordinate-method radiative transfer in multiple scattering and emitting layered media. *Appl. Opt.,* **27,** 2502–2509.

Stephens, G. L., 1984: The parameterization of radiation for numerical weather prediction and climate models. *Mon. Wea. Rev.,* **112,** 826–867.

——, S.-C. Tsay, P. W. Stackhouse Jr., and P. J. Flatau, 1990: The relevance of the microphysical and radiative properties of cirrus clouds to climatic feedback. *J. Atmos. Sci.,* **47,** 1742–1753.

Sykes, J. B., 1951: Approximate integration of the equation of transfer. *Mon. Not. R. Astron. Soc.,* **111,** 377–386.

Toon, O. B., C. P. McKay, and T. P. Ackerman, 1989: Rapid calculation of radiative heating rates and photodissociation rates in inhomogeneous multiple scattering atmospheres. *J. Geophys. Res.,* **94,** 16 287–16 301.

Tsay, S. C., K. Stamnes, and K. Jayaweera, 1989: Radiative energy budget in the cloudy and hazy arctic. *J. Atmos. Sci.,* **46,** 1002–1018.

Wiscombe, W. J., 1976: Extension of the doubling method to inhomogeneous sources. *J. Quant. Spectrosc. Radiat. Transfer,* **16,** 477–489.